

Topological black holes with curvature induced scalarization in the extended scalar-tensor theories

Stella Kiorpelidi,^{*} George Koutsoumbas,[†] Andri Machattou,[‡] and Eleftherios Papantonopoulos[§]
Physics Department, National Technical University of Athens, 15780 Zografou Campus, Athens, Greece

 (Received 18 February 2022; accepted 14 April 2022; published 18 May 2022)

We study the stability of topological black holes in the presence of a cosmological constant and a scalar field coupled to the Gauss-Bonnet (GB) term in the extended scalar-tensor theories. We find two competing effects. As the strength of the coupling λ of the scalar field to the GB term is increasing, the matter is interacting more strongly with gravity while as the hyperbolicity ξ of spacetime is getting larger the kinetic effects of matter tend to dominate. Calculating both analytically and numerically the quasinormal modes (QNMs) we found for each λ a critical value of ξ , below which there is an instability. When the coupling constant λ is getting very large, all of the QNMs develop a positive imaginary part indicating an instability. This behavior indicates a phase transition to a scalarized topological black hole induced by curvature effects.

DOI: [10.1103/PhysRevD.105.104039](https://doi.org/10.1103/PhysRevD.105.104039)

I. INTRODUCTION

The recent experimental results on gravitational waves [1–3] and more recently the observation of a shadow of the M87 black hole [4], demonstrated that Einstein’s general relativity (GR) is a very successful viable theory. However, on cosmological grounds, to explain the recent observational results on dark matter and on dark energy a generalization of GR is required, in an attempt to have a viable theory of gravity on short and large distances [5–8]. These modified gravity theories can give us important information on the structure and properties of the compact objects predicted by these theories and also the observational signatures, which they can introduce.

In particular, there has been a lot of activity in recent years in studding the astrophysical nature of compact objects. The direct observation of gravitational waves (GWs) produced by the collision of two compact objects stimulated this discussion. We expect that GW astronomy will deepen our understanding of the gravitational interaction and of astrophysics in extreme-gravity conditions. The future LIGO and Virgo observations will give us vital information on the structure of spacetime inside the light ring and then a strong gravity regime will gradually come into sight. The hope is to detect the postmerger ringdown phase that is produced by a series of damped oscillatory modes [9–11] which can be computed exactly in perturbation theory and to search for indications of new physics.

The modified GR theories predict theories with different properties of the near-horizon regions of black holes; therefore future GW observations will shed some light on the nature and the physics of these regions of black holes and see if they exhibit any unexpected structure. Alternatives to known black holes were recently constructed, known as exotic compact objects (ECOs) [12–14]. The important physical consequences of the existence of any structure at near-horizon scales would give rise to a series of “echoes” of the primary gravitational wave signal produced during the ringdown phase [15,16].

The ringdown waveform is dominated by the quasinormal modes (QNMs) [10,11,17] of the compact object under study. To determine the characteristic parameters of compact objects, the detection of a few modes from the ringdown signal is required. The ringdown signal is dominated by the photon sphere (PS) modes. These modes can be determined if the QNMs are known, while for ECOs, the PS modes still exist but there are not enough to determine the nature of these objects [15,16]. However, in [15,16] it was shown that the ringdown signal provides a conclusive proof for the formation of an event horizon or not. In these works it was shown that the ringdown waveform is dominated by the QNMs of the compact object producing waveforms in the form of echoes.

Some of the simplest and viable modifications of GR are the scalar-tensor theories [18]. When the scalar field coupled to gravity backreacts to the background metric, hairy black hole solutions would be generated. A hairy black hole solution in an asymptotically flat spacetime was found in [19] but it was shown that it was unstable because the scalar field was divergent on the event horizon [20]. However, it was soon realized that introducing a scale through the

^{*}stellakiorp@windowslive.com

[†]kutsbas@central.ntua.gr

[‡]andrimachattou@hotmail.com

[§]lpapa@central.ntua.gr

presence of a cosmological constant, making the spacetime asymptotically anti-de Sitter/de Sitter (AdS/dS), such an irregular behavior of the scalar field on the horizon was avoided. Then hairy black hole solutions were found having a regular scalar field behavior and all the possible divergences were hidden behind the horizon [21–31].

If the cosmological constant is positive and the scalar field is minimally coupled or nonminimally coupled with a self-interaction potential, black hole solutions were found [24,25,32] but it was shown to be unstable [26,33]. If the cosmological constant is negative, numerical solutions were found [27,28] and also a stable exact black hole solution was discussed in [23] in which the spacetime is asymptotically AdS with hyperbolic geometry, known as a Martinez-Troncoso-Zanelli (MTZ) black hole. Later this solution was generalized to include charge [34], while a generalization to nonconformal solutions was discussed in [30].

No-hair theorems can also be evaded by considering black holes interacting with matter fields [35–40]. In such cases black holes can support a nontrivial scalar field in their exterior region. Modified gravity theories were proposed in which matter is coupled to the Einstein tensor. These theories belong to general scalar-tensor Horndeski theories [41]. Then various hairy black holes were found in which scalar fields are coupled to curvature [31,42–50].

Hairy black hole solutions can also be obtained without the presence of matter sources if the scalar field is directly coupled to second-order algebraic curvature invariants. In this case the scalar hair is maintained by the interaction with the spacetime curvature. Exploring the strong field regime of gravity with the aim to detect gravitational waves and black hole shadows, the effects of higher-order curvature terms become significant. However, including such terms brings in the well-known ghost problem [51]. One high curvature correction is the Gauss-Bonnet (GB) term which is ghost-free but it becomes a topological term in four-dimensional spacetime and has no dynamics. To evade this problem, one has to couple this term to a scalar field in four dimensions [52]. These gravity theories are known as extended scalar-tensor-Gauss-Bonnet (ESTGB) theories and were studied extensively in the literature [53–58].

Recently there has been a lot of activity studying the ESTGB gravity theories in an attempt to evade the no-hair theorems and obtained hairy black hole solutions. In particular, for certain classes of the coupling function it was shown that we have spontaneous scalarization of black holes [59–64]. It was found that below a certain critical mass the Schwarzschild black hole becomes unstable in regions of strong curvature, and then when the scalar field backreacts to the metric, new branches of scalarized black holes develop at certain masses as solutions in the ESTGB theory [59,60,65]. An extension of these results is to consider the case of a nonzero black hole charge. Examining the entropy of the black holes with nontrivial scalar field it turned out that the solution with the scalar

field is thermodynamically favorable over the Reissner-Nordström one [66].

The spontaneous scalarization procedure has various applications. The scalarization due to a coupling of a scalar field to Ricci scalar was studied in [67] and scalarized black hole solutions and compact objects in asymptotical flat spacetime in the ESTGB gravity theories were obtained in [68–78] and also in AdS/dS spacetimes [79–83]. The connections of asymptotically AdS black hole scalarization with holographic phase transitions in the dual boundary theory were studied in [84,85]. Recently the spontaneous scalarization in $f(R)$ gravity theories was discussed in [86].

The black hole spontaneous scalarization in ESTGB gravity theories with a probe scalar field in a black hole background with different curvature topologies has been studied in [87]. It was found that the scalar field near an AdS black hole with positive curvature could be much easier to scalarize the black hole comparing with negative and zero curvature cases. In particular, when the curvature is negative, the scalar field is the most difficult to be bounded near the horizon. It was observed that scalarizations in hyperbolic AdS topological black hole (TBH) backgrounds depend on the interplay of two factors, the coupling strength between the scalar field and the GB term and the cosmological constant.

As we already mentioned, the MTZ black hole [23] is an exact black hole solution in four dimensions with a minimally coupled self-interacting scalar field, in an asymptotically AdS spacetime in which the event horizon is a surface of negative constant curvature enclosing the curvature singularity. It was shown that there is a second-order phase transition at a critical temperature below which a black hole in vacuum undergoes a spontaneous dressing up with a nontrivial scalar field. In a series of papers [88–90] this scalarization procedure was studied for topological black holes. Calculating analytically and numerically the QNMs of tensor, electromagnetic and scalar perturbations, it was found that there is a critical value of the horizon radius below which the topological black hole is scalarized to the MTZ black hole with scalar hair. The thermodynamics of this transition was also studied.

Motivated by the above studies we will study the scalarization of a topological black hole in the presence of the coupling of the scalar field to the GB term in the ESTGB gravity theories. In particular, we will consider a gravity theory with the presence of a cosmological constant in which there is matter parametrized by a massive scalar field minimally coupled to gravity and also coupled to the GB term. The coupling of the scalar field to the GB term is denoted by the parameter λ . At first the scalar field does not backreact to the metric. We fix the background metric to be a TBH leaving in a hyperbolic spacetime expressed by a parameter ξ , which is analogous of the orbital quantum number in the three-dimensional space.

The goal of this work is to study the behavior of matter in this physical setup. For a fixed cosmological constant we

have two competing effects. The first one is that as λ is increasing we expect the matter to interact more strongly with gravity, while as ξ is getting larger the kinetic effects tend to dominate. We calculate both analytically and numerically the QNMs of scalar perturbations of topological-AdS black holes in the presence of matter coupled to the GB term. For each λ we found a critical value of ξ , below which there is instability. As λ is increasing the imaginary part of some QNMs are getting positive indicating an instability. When the coupling constant λ is getting very large, all of the QNMs develop a positive imaginary part. This behavior provides evidence of a phase transition to a scalarized TBH. We also noted that the absolute values of QNMs are increasing as the parameter ξ is also increasing.

This behavior of the parameters λ and ξ gives us information about the matter distribution near the horizon of the TBH. In [91] the behavior of matter outside the horizon of a compact object described by a hairy black hole in the Horndeski theory was studied. It was shown that echoes were formed in the ringdown waveform due to the entrapment of test fields between the photon sphere and the effective asymptotic boundary. Also it was found that the stability of the compact object produces decaying echoes modes, while instability generates growing echoes modes. In a future work it would be interesting to study the echoes that are generated in a scalarized topological black hole and see what kind of observational signals can be produced by the interplay of the strength of the coupling of matter to curvature and the form of the topology of the spacetime.

The work is organized as follows. In Sec. II we present the theory of the coupling of a scalar field to the GB term in the background of a TBH and we discuss the tachyonic instabilities of this theory. In Sec. III we carry out an analytical calculation of QNMs. In Sec. IV we consider scalar perturbations in the extended scalar-tensor GB theory in which the background metric is the TBH and finally in Sec. V are our conclusions.

II. TOPOLOGICAL BLACK HOLES, THE EINSTEIN-SCALAR-GAUSS-BONNET THEORY AND TACHYONIC INSTABILITIES

In this section we will first discuss the TBHs as the background of the scalar-GB gravity theories and then we will discuss the possible tachyonic instabilities of these theories.

We consider the bulk action

$$I = \frac{1}{16\pi G} \int d^4x \sqrt{-g} \left[R + \frac{6}{l^2} \right], \quad (2.1)$$

in asymptotically AdS spacetime, where G is Newton's constant and l is the AdS radius. The presence of a negative cosmological constant ($\Lambda = -\frac{3}{l^2}$) allows the existence of black holes with a topology $\mathbb{R} \times \Sigma$, where Σ is

a two-dimensional manifold of constant negative curvature. These black holes are known as topological black holes. The simplest solution of this kind reads

$$ds^2 = -g(r)dt^2 + \frac{dr^2}{g(r)} + r^2 d\sigma^2, \\ g(r) = r^2 - 1 - \frac{2\mu}{r}, \quad (2.2)$$

where we employed units in which the AdS radius is $l = 1$ and $d\sigma$ is the line element of Σ . The latter is locally isomorphic to the hyperbolic manifold H^2 and of the form

$$\Sigma = H^2/\Gamma, \quad \Gamma \subset O(2, 1), \quad (2.3)$$

where Γ is a freely acting discrete subgroup (i.e. without fixed points) of isometries.

The geometry of the TBHs as well their basic properties have been studied extensively in the literature [92–96]. It has been shown in [97] that the massless configurations where Σ has negative constant curvature are stable under gravitational perturbations. The stability also of the TBHs was discussed in [98] and QNMs in topological black holes were calculated in [99–101].

The Einstein-scalar-Gauss-Bonnet theory is described by the following action functional:

$$S = \frac{1}{16\pi G_N} \int d^4x \sqrt{-g} [R - 2\nabla_\mu \phi \nabla^\mu \phi - m^2 \phi^2 \\ + \lambda^2 f(\phi) \mathcal{R}_{GB}^2 - 2\Lambda]. \quad (2.4)$$

This modified gravitational theory consists of a real scalar field minimally coupled to Einstein's gravity and non-minimally coupled to the quadratic gravitational GB term \mathcal{R}_{GB}^2 through a real function $f(\phi)$. A cosmological constant Λ is also present, which may take either a positive or a negative value. We are interested in hyperbolic TBHs with negative curvature constant. So the metric ansatz reads as

$$ds^2 = -e^{A(r)} dt^2 + e^{B(r)} dr^2 + r^2 (d\theta^2 + \sinh^2 \theta d\phi^2). \quad (2.5)$$

Using natural units such that $G_N = c = 1$ the gravitational field equations have the covariant form

$$G_{\mu\nu} = \tilde{T}_{\mu\nu}, \quad (2.6)$$

$$G_{\mu\nu} = T_{\mu\nu}^{(\phi)} + T_{\mu\nu}^{(GB)} - \Lambda g_{\mu\nu}, \quad (2.7)$$

$$G_{\mu\nu} + \Lambda g_{\mu\nu} = T_{\mu\nu}^{(\phi)} + T_{\mu\nu}^{(GB)}, \quad (2.8)$$

where $G_{\mu\nu}$ is the Einstein tensor

$$G_{\mu\nu} = R_{\mu\nu} - \frac{1}{2} g_{\mu\nu} R, \quad (2.9)$$

and $T_{\mu\nu}^{(\phi)}$ is the energy-momentum tensor which receives contribution only from the kinetic term and the mass term of the scalar field, and $T_{\mu\nu}^{(\text{GB})}$ is the energy-momentum tensor which receives contribution only from the interaction of the scalar field with the Gauss-Bonnet term

$$T_{\mu\nu}^{(\phi)} = -\frac{1}{2}g_{\mu\nu}m^2\phi^2 + 2\nabla_\mu\phi\nabla_\nu\phi - g_{\mu\nu}\nabla_\kappa\phi\nabla^\kappa\phi, \quad (2.10)$$

$$\begin{aligned} T_{\mu\nu}^{(\text{GB})} &= -R(\nabla_\mu\Psi_\nu + \nabla_\nu\Psi_\mu) - 4\nabla^\alpha\Psi_\alpha G_{\mu\nu} \\ &+ 4R_{\mu\alpha}\nabla^\alpha\Psi_\nu + 4R_{\nu\alpha}\nabla^\alpha\Psi_\mu - 4g_{\mu\nu}R^{\alpha\beta}\nabla_\alpha\Psi_\beta, \\ &+ 4R^\beta_{\mu\alpha\nu}\nabla^\alpha\Psi_\beta, \end{aligned} \quad (2.11)$$

with

$$\Psi_\mu = \lambda^2\dot{f}(\phi)\nabla_\mu\phi. \quad (2.12)$$

The equation of motion of the scalar field is

$$\nabla_\mu\nabla^\mu\phi - \frac{1}{2}m^2\phi + \frac{1}{4}\lambda^2\dot{f}(\phi)\mathcal{R}_{\text{GB}}^2 = 0, \quad (2.13)$$

where the dot denotes differentiation with respect to the scalar field. A condition for the coupling function $f(\phi)$ arises from Eq. (2.13), namely $\dot{f}(0) = 0$. This condition ensures that the trivial scalar field ($\phi = 0$) satisfies the equation of motion. In the case of a trivial scalar field the metric functions of the background TBH are given by

$$e^{A(r)} \equiv g(r) = -1 - \frac{M}{r} - \frac{\Lambda}{3}r^2, \quad (2.14)$$

$$e^{B(r)} = \frac{1}{-1 - \frac{M}{r} - \frac{\Lambda}{3}r^2} = \frac{1}{g(r)}. \quad (2.15)$$

The equation of motion of the scalar field (2.13) can be written as

$$(\square - \mu_{\text{eff}}^2)\phi = 0, \quad (2.16)$$

where

$$\mu_{\text{eff}}^2 = \frac{1}{2}m^2 - \frac{1}{4}\lambda^2\dot{f}(\phi)\mathcal{R}_{\text{GB}}^2. \quad (2.17)$$

The sign of this effective mass is connected with the stability or instability of the underlining theory. To clarify this issue, consider the Lagrangian density for a free relativistic scalar field ϕ in a Minkowski spacetime

$$\mathcal{L} = -\frac{\epsilon}{2}\partial_\mu\phi\partial^\mu\phi - \frac{\epsilon}{2}m^2\phi^2. \quad (2.18)$$

In the $\epsilon = \epsilon = +1$ case, the Hamiltonian is positive semi-definite and therefore bounded from below, while in the

$\epsilon = \epsilon = -1$ case, the Hamiltonian is negative semidefinite and therefore bounded from above. In the case $\epsilon = -\epsilon$, the Hamiltonian is indefinite and so it is not bounded either from below or from above. The field ϕ is called a ghost field if $\epsilon = \epsilon = -1$ (for a review on ghost fields see [102]), while it is called a tachyon field if $\epsilon = +1$ and $\epsilon = -1$, and finally, it is called a tachyonic ghost if $\epsilon = -1$ and $\epsilon = +1$. A Hamiltonian that is unbounded from below is usually associated with instabilities of the system. If $\epsilon = -\epsilon$, a small perturbation can grow exponentially, signaling an instability.

If the effective mass (2.17) is negative $\mu_{\text{eff}}^2 < 0$, there is a tachyonic instability triggered by a negative effective mass squared of the scalar field [80].

III. ANALYTICAL CALCULATION OF QNMs

We consider a function $f(\phi)$ coupled to the GB term, for which

$$\left.\frac{df}{d\phi}\right|_{\phi=0} = 0, \quad \left.\frac{d^2f}{d\phi^2}\right|_{\phi=0} = 2 > 0. \quad (3.1)$$

We suppose that ϕ is restricted in the well surrounding $\phi = 0$, so that the expression $\lambda^2 f(\phi)\mathcal{R}_{\text{GB}(0)}^2$ reduces in this limit to the approximate form $\lambda^2\mathcal{R}_{\text{GB}(0)}^2\phi^2$. We consider the line element

$$\begin{aligned} ds^2 &= -g(r)dt^2 + \frac{1}{g(r)}dr^2 + r^2(d\theta^2 + \sin^2\theta d\phi^2), \\ g(r) &= -1 - \frac{M}{r} - \frac{\Lambda}{3}r^2 = -1 - \frac{M}{r} + \frac{r^2}{L^2}, \end{aligned} \quad (3.2)$$

for which the GB invariant reads

$$\mathcal{R}_{\text{GB}(0)}^2 = \frac{24}{L^4} + \frac{12M^2}{r^6}. \quad (3.3)$$

The starting point of our approach will be an equation describing the scalar perturbations, which derives from the Klein-Gordon equation after substituting for the scalar field the form

$$\phi(t, r, \theta, \phi) = \Psi(r)e^{-i\omega t}\mathcal{Y}_{\xi m}(\theta, \phi), \quad (3.4)$$

where $\mathcal{Y}_{\xi m}(\theta, \phi)$ are the counterparts of the spherical harmonics and ξ is a parameter analogous to the orbital quantum number. The equation reads

$$\begin{aligned} g(r)\frac{d}{dr}\left(g(r)\frac{d\Psi}{dr}\right) + [\omega^2 - \mathcal{V}(r)]\Psi &= 0, \\ \mathcal{V}(r) \equiv g(r)\left[\frac{g'(r)}{r} - \frac{\lambda^2}{4}\mathcal{R}_{\text{GB}(0)}^2 + \frac{\xi^2 + \frac{1}{4}}{r^2}\right]. \end{aligned} \quad (3.5)$$

Note that the parameter ξ indicates the hyperbolic geometry. A large value of ξ shows the departure from the spherical topology.

Substituting $g(r)$ and $\mathcal{R}_{\text{GB}(0)}^2$ by their respective values, Eq. (3.5) takes the form

$$g(r) \frac{d}{dr} \left(g(r) \frac{d\Psi}{dr} \right) + \left[\omega^2 - g(r) \left(\frac{2}{L^2} + \frac{M}{r^3} - \frac{6\lambda^2}{L^4} - \frac{3\lambda^2 M^2}{r^6} + \frac{\xi^2 + \frac{1}{4}}{r^2} \right) \right] \Psi = 0. \quad (3.6)$$

We now introduce the new variable

$$u \equiv \left(\frac{r_+}{r} \right)^2 \Leftrightarrow r = \frac{r_+}{u^{1/2}}, \quad (3.7)$$

so that

$$\frac{d}{dr} = -\frac{2u^{3/2}}{r_+} \frac{d}{du}, \quad \frac{d^2}{dr^2} = \frac{4}{r_+^2} u^{3/2} \frac{d}{du} \left(u^{3/2} \frac{d}{du} \right), \quad (3.8)$$

and Eq. (3.6) becomes

$$\frac{4}{r_+^2} g u^{3/2} \frac{d}{du} \left(g u^{3/2} \frac{d}{du} \right) \Psi + \left[\omega^2 - g \left(2 + \frac{M u^{3/2}}{r_+^3} - 6\lambda^2 - \frac{3\lambda^2 M^2 u^3}{r_+^6} + \frac{\xi^2 + \frac{1}{4}}{r_+^2} u \right) \right] \Psi = 0. \quad (3.9)$$

Setting $L = 1$ and using the notations

$$\hat{g}(u) \equiv \frac{g(r)}{r_+^2} = \frac{1}{u} - \frac{1}{r_+^2} - \frac{M}{r_+^3} u^{1/2}, \quad (3.10)$$

$$\begin{aligned} \hat{\mathcal{V}}(u) &\equiv \frac{\mathcal{V}(r)}{r_+^2} \\ &= \hat{g}(u) \left[2 + \frac{M u^{3/2}}{r_+^3} - 6\lambda^2 - \frac{3\lambda^2 M^2 u^3}{r_+^6} + \frac{\xi^2 + \frac{1}{4}}{r_+^2} u \right], \end{aligned} \quad (3.11)$$

the equation takes the form

$$\begin{aligned} -4u^{3/2} \hat{g}(u) (u^{3/2} \hat{g}(u) \Psi')' + \hat{\mathcal{V}} \Psi &= \hat{\omega}^2 \Psi \\ \Leftrightarrow H \Psi = \hat{\omega}^2 \Psi, \quad \hat{\omega} &\equiv \frac{\omega}{r_+}. \end{aligned} \quad (3.12)$$

It is possible to proceed with an analytical approach, in two cases, namely when the black hole is small with r_+ around 1 or when the black hole is large.

A. Small black hole: The horizon is approximately 1

We now restrict our attention to the critical case, where

$$r_+ = 1 \Leftrightarrow M = 0.$$

In this case

$$\hat{g}(u) = \frac{1-u}{u},$$

and the equation reduces to

$$\begin{aligned} -4u^{1/2} \hat{g}(u) (u^{1/2} (1-u) \Psi')' + \hat{\mathcal{V}}(u) \Psi &= \frac{\hat{\omega}^2}{1-u} \Psi \\ \Leftrightarrow H \Psi = \frac{\hat{\omega}^2}{1-u} \Psi, \end{aligned} \quad (3.13)$$

with

$$\hat{\mathcal{V}}(u) = \frac{2-6\lambda^2}{u} + \left(\xi^2 + \frac{1}{4} \right),$$

and then the Klein-Gordon equation becomes

$$-4u^{1/2} (u^{1/2} (1-u) \Psi')' + \left(\frac{2-6\lambda^2}{u} + \xi^2 + \frac{1}{4} \right) \Psi = \frac{\hat{\omega}^2}{1-u} \Psi. \quad (3.14)$$

We introduce the parameter $a \equiv 2-6\lambda^2$, so that the potential takes on the simple form

$$\hat{\mathcal{V}} = \frac{a}{u} + \xi^2 + \frac{1}{4},$$

and the equation to be solved reads

$$\begin{aligned} 4(1-u)u\Psi'' + 2(1-u)\Psi' - 4u\Psi' + \frac{\hat{\omega}^2}{1-u}\Psi \\ - \left(\frac{a}{u} + \xi^2 + \frac{1}{4} \right) \Psi = 0. \end{aligned} \quad (3.15)$$

One may check that the (finite) approximate solution in the limit $u \rightarrow 0$ is proportional to $u^{\frac{1+\sqrt{1+4a}}{4}}$, while in the limit $u \rightarrow 1$ it is proportional to $(1-u)^{\pm \frac{i\omega}{2}}$. We choose $(1-u)^{-\frac{i\omega}{2}}$, in which case a negative imaginary part of ω corresponds to a stable system. It is convenient to make the transformation

$$\Psi(u) = u^{\frac{1+\sqrt{1+4a}}{4}} (1-u)^{-\frac{i\omega}{2}} X(u). \quad (3.16)$$

The function $X(u)$ interpolates between the two limiting values of $u \rightarrow 1$ and $u \rightarrow 0$. Then the differential equation becomes

$$16u(1-u)X''(u) + 8[-2 - \sqrt{1+4a} + u(4 + \sqrt{1+4a} - 2i\omega)]X'(u) + [5 + 4a + 4\sqrt{1+4a} + 4\xi^2 - 8i\omega - 4i\sqrt{1+4a}\omega - 4\omega^2]X(u) = 0, \tag{3.17}$$

which may be readily solved in terms of hypergeometric functions

$$X(u) = C_{12}F_1\left(\frac{1}{2} + \frac{\sqrt{1+4a}}{4} - \frac{i\xi}{2} - \frac{i\omega}{2}, \frac{1}{2} + \frac{\sqrt{1+4a}}{4} + \frac{i\xi}{2} - \frac{i\omega}{2}, 1 + \frac{\sqrt{1+4a}}{2}, u\right) + C_2u^{-\frac{\sqrt{1+4a}}{2}}{}_2F_1\left(\frac{1}{2} - \frac{\sqrt{1+4a}}{4} - \frac{i\xi}{2} - \frac{i\omega}{2}, \frac{1}{2} - \frac{\sqrt{1+4a}}{4} + \frac{i\xi}{2} - \frac{i\omega}{2}, 1 - \frac{\sqrt{1+4a}}{2}, u\right). \tag{3.18}$$

Thus one obtains the solution of the original equation

$$\Psi(u) = C_1u^{\frac{1+\sqrt{1+4a}}{4}}(1-u)^{-\frac{i\omega}{2}}{}_2F_1\left(\frac{1}{2} + \frac{\sqrt{1+4a}}{4} - \frac{i\xi}{2} - \frac{i\omega}{2}, \frac{1}{2} + \frac{\sqrt{1+4a}}{4} + \frac{i\xi}{2} - \frac{i\omega}{2}, 1 + \frac{\sqrt{1+4a}}{2}, u\right) + C_2u^{\frac{1-\sqrt{1+4a}}{4}}(1-u)^{-\frac{i\omega}{2}}{}_2F_1\left(\frac{1}{2} - \frac{\sqrt{1+4a}}{4} - \frac{i\xi}{2} - \frac{i\omega}{2}, \frac{1}{2} - \frac{\sqrt{1+4a}}{4} + \frac{i\xi}{2} - \frac{i\omega}{2}, 1 - \frac{\sqrt{1+4a}}{2}, u\right). \tag{3.19}$$

In view of the above expressions when $1 + 4a = 0$ we get a critical value for the GB coupling

$$\lambda_c = \sqrt{\frac{3}{8}} \approx 0.61.$$

If λ is small enough, i.e. $\lambda < \lambda_c$, one should set $C_2 = 0$ to ensure finiteness at $u \rightarrow 0$. The solution reduces to

$$\Psi(u) = C_1u^{\frac{1+\sqrt{1+4a}}{4}}(1-u)^{-\frac{i\omega}{2}} \times {}_2F_1\left(\frac{1}{2} + \frac{\sqrt{1+4a}}{4} - \frac{i\xi}{2} - \frac{i\omega}{2}, \frac{1}{2} + \frac{\sqrt{1+4a}}{4} + \frac{i\xi}{2} - \frac{i\omega}{2}, 1 + \frac{\sqrt{1+4a}}{2}, u\right). \tag{3.20}$$

The expansion of the hypergeometric function around $u = 1$ reads

$${}_2F_1\left(\frac{1}{2} + \frac{\sqrt{1+4a}}{4} - \frac{i\xi}{2} - \frac{i\omega}{2}, \frac{1}{2} + \frac{\sqrt{1+4a}}{4} + \frac{i\xi}{2} - \frac{i\omega}{2}, 1 + \frac{\sqrt{1+4a}}{2}, u\right) \simeq K_1 \frac{1}{\Gamma\left(\frac{1}{2} + \frac{\sqrt{1+4a}}{4} - \frac{i\xi}{2} + \frac{i\omega}{2}\right)\Gamma\left(\frac{1}{2} + \frac{\sqrt{1+4a}}{4} + \frac{i\xi}{2} + \frac{i\omega}{2}\right)\Gamma(1-i\omega)} + K_2 \frac{1}{\Gamma\left(\frac{1}{2} + \frac{\sqrt{1+4a}}{4} - \frac{i\xi}{2} - \frac{i\omega}{2}\right)\Gamma\left(\frac{1}{2} + \frac{\sqrt{1+4a}}{4} + \frac{i\xi}{2} - \frac{i\omega}{2}\right)\Gamma(1+i\omega)} (1-u)^{+i\omega}, \tag{3.21}$$

where K_1 and K_2 are constants, in the sense that they do not involve u . Since we insist on having only terms of the form $(1-u)^{-\frac{i\omega}{2}}$ near $u = 1$, it is obvious that the second term, which involves $(1-u)^{+i\omega}$, should be discarded; the only way to discard it is the divergence to infinity of the Γ functions in the denominator, which happens when

$$\frac{1}{2} + \frac{\sqrt{1+4a}}{4} + \frac{i\xi}{2} - \frac{i\omega}{2} = -n, \Rightarrow \omega = \pm\xi - i\left(2n + \frac{2 + \sqrt{1+4a}}{2}\right). \tag{3.22}$$

The quantity n is a non-negative integer. Thus we have determined (to zeroth approximation) the QNMs

$$\omega_n = \pm\xi - i\left(2n + \frac{2 + \sqrt{9 - 24\lambda^2}}{2}\right), \quad n=0,1,2,\dots \quad (3.23)$$

for small GB coupling λ , less than its critical value λ_c .

If λ grows enough, so that $\lambda > \lambda_c$, we work along similar lines and we get

$$\omega_n = \pm\xi + \frac{\sqrt{24\lambda^2 - 9}}{2} - i(2n + 1). \quad (3.24)$$

Notice that the real part of the QNMs may be nonzero even when ξ vanishes.

1. Analytical predictions for the QNMs

The above analysis holds strictly at $r_+ = 1$. Thus we have a prediction for the results if $r_+ = 1$:

- (i) For small λ we expect to find QNMs $\omega \equiv \omega_R - i\omega_I$ with a constant $\omega_R = \pm\xi$ (the same for all of them) and with ω_I , with an interval 2 between successive values.
- (ii) For large λ we expect $\omega_R = \pm\xi + \frac{\sqrt{24\lambda^2 - 9}}{2}$.

One may depict the above changes in Fig. 1, where the quantities ω_R and ω_I are shown versus λ . It is evident that a qualitative change happens at $\lambda = \lambda_c$, since the slope presents a discontinuity. It is reasonable to expect a phase transition to happen at this value of λ . The real part ω_R vanishes for small λ , that is $\lambda < \lambda_c$, while it takes nonzero values for large λ , even though ξ is set to zero. In addition, it does not depend on the integer n . On the other hand, the imaginary part ω_I depends on the integer n .

In the numerical calculations of the QNMs one works actually for values for r_+ either slightly smaller or slightly larger than 1. In [90] it was found that the real part for $r_+ \neq 1$ is no more the same for all QNMs, as predicted above, there is a slope, which is positive (negative) for $r_+ < 1$ ($r_+ > 1$). Thus the QNMs are infinite in number for $r_+ > 1$, while for $r_+ < 1$ the QNMs approach the vertical

axis and eventually cease to exist. In addition, if ξ is small enough, no propagating modes exist.

From Fig. 1 we can see that for $\lambda < \lambda_c$, the real part of the QNMs is zero, while the imaginary part is negative. These results indicate that for values of λ below its critical value the TBH is stable under scalar perturbations, while above that critical value of λ we have instability, indicating that we have a phase transition of the TBH to a MTZ-like black hole.

If we want to go to different (but close enough) values of r_+ , we may calculate corrections analytically, using perturbation theory. However, this is technically difficult, so we postpone it for a future work. We expect that instabilities may show up in a perturbative calculation for $r_+ \neq 1$, when λ takes on sufficiently large values.

We have not been able to analytically investigate the regime of very small ($r_+ \ll 1$) or very large ($r_+ \gg 1$) black holes. However, the numerical results that we present in later sections indicate that there are no QNMs for either of these categories of black holes. Thus it is plausible that only horizons around $r_+ \approx 1$ may be expected to yield QNMs.

B. Scalar modes

To calculate the scalar modes we start with Eq. (3.14) when the horizon equals 1,

$$-4u^{1/2}(u^{1/2}(1-u)\Psi')' + \left(\frac{2-6\lambda^2}{u} + \xi^2 + \frac{1}{4}\right)\Psi = \frac{\hat{\omega}_n^2}{1-u}\Psi. \quad (3.25)$$

We employ the transformation (3.16)

$$\Psi(u) = u^{\frac{1+\sqrt{9-24\lambda^2}}{4}}(1-u)^{-\frac{i\omega_n}{2}}X(u), \quad (3.26)$$

and use the result (3.22)

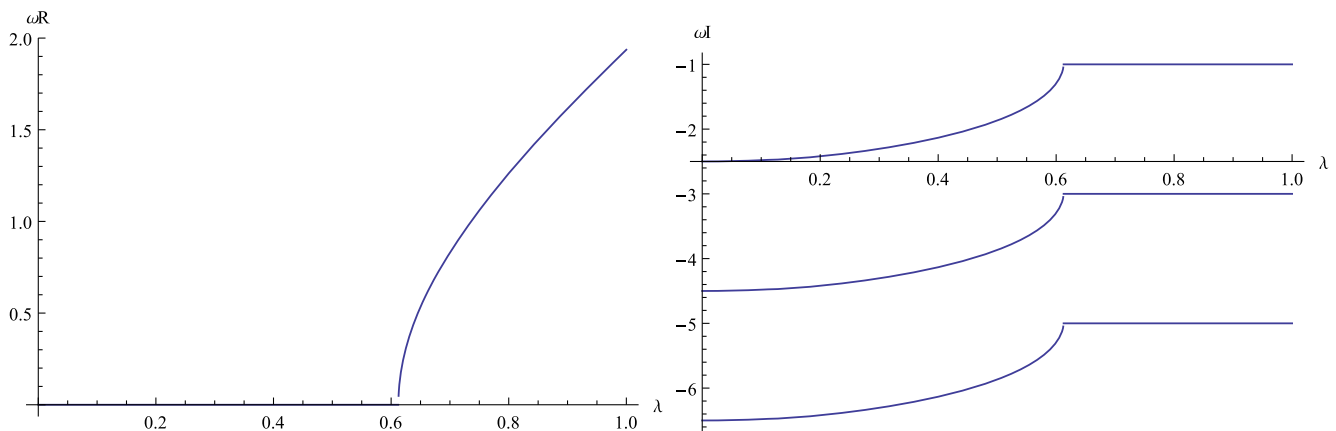


FIG. 1. ω_R (left) and ω_I (right) versus λ for $\xi = 0$ and $n = 0, 1$ and 2 . The value $n = 0$ corresponds to the uppermost curve.

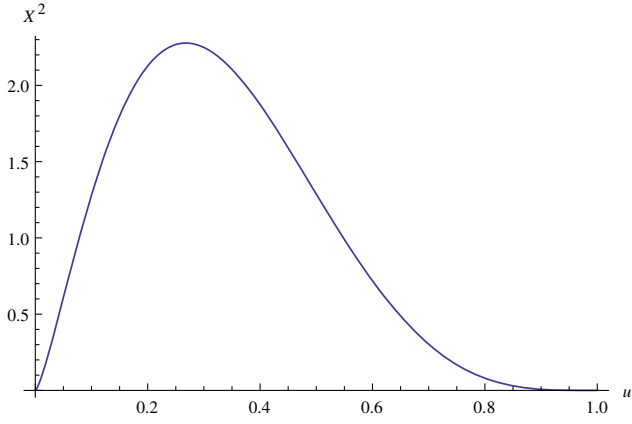


FIG. 2. $X^*(u)X(u)$ for the scalar field versus u for $\lambda = 0.5$ and $\xi = 0$.

$$\omega_n = \pm\xi - i\left(2n + \frac{2 + \sqrt{9 - 24\lambda^2}}{2}\right). \quad (3.27)$$

The resulting equation reads

$$2(-1 + u)uX'' + [2 + \sqrt{9 - 24\lambda^2} + u(-2 + 4n + 2i\xi)]X' + 2n(n + i\xi)X = 0. \quad (3.28)$$

Let us check the behavior of the quantity

$$\hat{\rho} = \Psi^*(u)\Psi(u), \quad (3.29)$$

which contains the u dependence of the charge density

$$\rho = \frac{e}{2m} [(\Psi e^{-i\omega t})^* \partial_t (\Psi e^{-i\omega t}) - (\Psi e^{-i\omega t}) \partial_t (\Psi e^{-i\omega t})^*]_{t=0}. \quad (3.30)$$

For $n = 0$ the equation simplifies to

$$2(-1 + u)uX'' + [2 + \sqrt{9 - 24\lambda^2} + u(-2 + 2i\xi)]X' = 0. \quad (3.31)$$

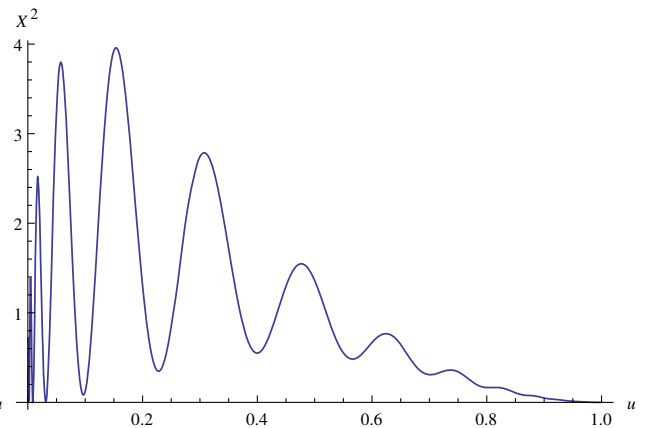
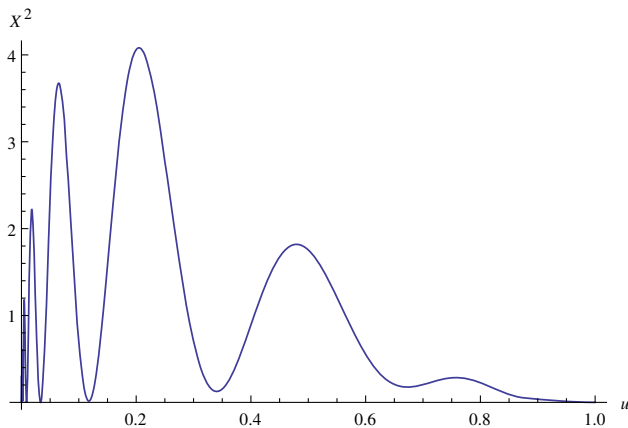


FIG. 3. $X^*(u)X(u)$ for the scalar field versus u for $\lambda = 2.0$ and either $\xi = 0$ (left) or $\xi = 10$ (right).

The solution reads

$$X = c_1 + c_2 u^{-\frac{1}{2}\sqrt{9-24\lambda^2}} {}_2F_1\left(-\frac{1}{2}\sqrt{9-24\lambda^2}, -\frac{1}{2}\sqrt{9-24\lambda^2} - i\xi, -\frac{1}{2}\sqrt{9-24\lambda^2}, u\right). \quad (3.32)$$

However, the factor $u^{-\frac{1}{2}\sqrt{9-24\lambda^2}}$ does not behave properly in the limit $u \rightarrow 0$, if $\lambda < \lambda_c$, so, in this case, the result is a constant function, that is, c_2 must be set to zero. Thus the solution for $\lambda < \lambda_c$ takes the form

$$\Psi_{<}(u) = c_1 u^{\frac{1+\sqrt{9-24\lambda^2}}{4}} (1-u)^{-\frac{i\omega}{2}}, \quad \omega = \pm\xi - i\frac{2 + \sqrt{9-24\lambda^2}}{2}. \quad (3.33)$$

Its solution for $\lambda > \lambda_c$ is the linear combination

$$\Psi_{>}(u) = u^{\frac{1}{4}} u^{\frac{i\sqrt{24\lambda^2-9}}{4}} (1-u)^{-\frac{i\omega_n}{2}} \quad (3.34)$$

$$\times \left[c_1 + c_2 u^{-\frac{i}{2}\sqrt{24\lambda^2-9}} {}_2F_1\left(-\frac{i}{2}\sqrt{24\lambda^2-9}, -\frac{i}{2}\sqrt{24\lambda^2-9} - i\xi, -\frac{i}{2}\sqrt{24\lambda^2-9}, u\right) \right], \quad (3.35)$$

$$\omega_n = \pm\left(\xi + \frac{\sqrt{24\lambda^2-9}}{2}\right) - i(2n+1). \quad (3.36)$$

We set $\lambda = 0.5$, which lies in the region of small λ values. We may check by inspection that there is no dependence on ξ in this region of λ (and in this approximation). Figure 2 displays the result.

In Fig. 3 one may observe the results for $\lambda = 2.0$, that is $\lambda > \lambda_c$, at $\xi = 0$ and $\xi = 10$. The most striking characteristic is the qualitative difference between Figs. 2 and 3 (left panel), which may lend support to the conjecture that moving to large values of λ may result in a phase transition.

When one uses $\xi = 10$, quantitative differences are evident, in contrast to the previous case, but these differences do not qualify for a qualitative change.

IV. SCALAR PERTURBATIONS

In this section we will consider scalar perturbation in ESTGB gravity theories in the case where the background metric is the TBH. In the case of a trivial scalar field, the equation which describes massive scalar perturbations in this spacetime background reads

$$\left(\square_{(0)} - \frac{m^2}{2} + \frac{1}{4} \lambda^2 \mathcal{R}_{\text{GB}(0)}^2 \right) \delta\phi = 0, \quad (4.1)$$

where $\square_{(0)}$ and $\mathcal{R}_{\text{GB}(0)}^2$ are the D'Alembert operator and the Gauss-Bonnet invariant for the topological geometry. So

$$\begin{aligned} \mathcal{R}_{\text{GB}(0)}^2 &= \frac{4((g(r) + 1)g''(r) + g'(r)^2)}{r^2} \\ &= \frac{24}{L^4} + \frac{12M^2}{r^6}. \end{aligned} \quad (4.2)$$

This small perturbation has the same symmetries of the TBH, namely static and spherical symmetry. So the variables can be decomposed by the standard way

$$\delta\phi = u(r) e^{-i\omega t} \mathcal{Y}_{\xi m}(\theta, \varphi). \quad (4.3)$$

Note that the spherical harmonics $\mathcal{Y}_{\xi m}(\theta, \varphi)$ obey the equation

$$\begin{aligned} \frac{1}{\sinh \theta} \partial_\theta (\sinh \theta \partial_\theta \mathcal{Y}_{\xi m}(\theta, \varphi)) + \frac{1}{\sinh^2 \theta} \partial_\phi^2 \mathcal{Y}_{\xi m}(\theta, \varphi) \\ = - \left(\xi^2 + \frac{1}{4} \right) \mathcal{Y}_{\xi m}(\theta, \varphi). \end{aligned} \quad (4.4)$$

After substituting in Eq. (4.1) and introducing the tortoise coordinate $dr^* = \frac{1}{g(r)} dr$, we obtain the following Schrödinger-like equation:

$$u''(r^*) + (\omega^2 - \mathcal{U}(r))u(r^*) = 0, \quad (4.5)$$

where the effective potential $\mathcal{U}(r)$ reads

$$\mathcal{U}(r) = g(r) \left(\frac{1}{2} m^2 + \frac{1}{r} g'(r) - \frac{\lambda^2}{4} \mathcal{R}_{\text{GB}(0)}^2 + \frac{\xi^2 + \frac{1}{4}}{r^2} \right), \quad (4.6)$$

and using (4.2) we have

$$\begin{aligned} \mathcal{U}(r) &= \left(-1 - \frac{M}{r} + \frac{r^2}{L^2} \right) \left(\frac{1}{2} m^2 + \frac{1}{r} \left(\frac{M}{r^2} + \frac{2r}{L^2} \right) \right. \\ &\quad \left. - \frac{\lambda^2}{4} \left(\frac{24}{L^4} + \frac{12M^2}{r^6} \right) + \frac{\xi^2 + \frac{1}{4}}{r^2} \right). \end{aligned} \quad (4.7)$$

In the case of a nontrivial scalar field (2.12) the wave equation reads

$$-\frac{1}{\sqrt{-g}} \partial_\mu [\sqrt{-g} g^{\mu\nu} \partial_\nu \Psi] + \frac{dU}{d\Psi} = 0. \quad (4.8)$$

In the TBH background we have

$$\begin{aligned} \frac{1}{\sqrt{-g}} \partial_\mu [\sqrt{-g} g^{\mu\nu} \partial_\nu \Psi] &= -\frac{1}{g(r)} \partial_{tt} \Psi + \frac{1}{r^2} \partial_r [r^2 g(r) \partial_r \Psi] \\ &\quad + \frac{1}{r^2} \frac{1}{\sinh \theta} \partial_\theta [\sinh \theta \partial_\theta \Psi] \\ &\quad + \frac{1}{r^2 \sinh^2 \theta} \partial_\phi^2 \Psi. \end{aligned}$$

On the other hand, for the spherical harmonics $\mathcal{Y}_q^{(k)}$ we have

$$\frac{1}{\sinh \theta} \partial_\theta [\sinh \theta \partial_\theta \mathcal{Y}_q^{(k)}] + \frac{1}{\sinh^2 \theta} \partial_\phi^2 \mathcal{Y}_q^{(k)} = - \left(\xi^2 + \frac{1}{4} \right) \mathcal{Y}_q^{(k)}, \quad (4.9)$$

while the potential reads

$$U = \frac{1}{2} m^2 \Psi^2 - \frac{\lambda^2}{2} f(\Psi) R_{\text{GB}}^2, \quad (4.10)$$

where

$$\begin{aligned} R_{\text{GB}}^2 &= R^2 - 4R_{\mu\nu} R^{\mu\nu} + R_{\mu\nu\alpha\beta} R^{\mu\nu\alpha\beta} \\ &\rightarrow \frac{4}{r^2} [g'^2(r) + (g(r) + 1)g''(r)], \end{aligned} \quad (4.11)$$

so that, replacing $\Psi(t, r, \theta, \phi) = \Phi(t, r) \mathcal{Y}_q^{(k)}(\theta, \phi)$, one ends up with an equation for a field depending just on t and r ,

$$\begin{aligned} \frac{1}{g(r)} \partial_{tt} \Phi(t, r) - \frac{1}{r^2} \partial_r [r^2 g(r) \partial_r \Phi(t, r)] + \frac{\xi^2 + \frac{1}{4}}{r^2} \Phi \\ + m^2 \Phi(t, r) - \lambda^2 R_{\text{GB}}^2 \frac{dF}{d\Phi} = 0. \end{aligned} \quad (4.12)$$

If we fix the scalar function to $F = \frac{1}{2} \Phi^2$, the scalar field equation becomes

$$\begin{aligned} \frac{1}{g(r)} \partial_{tt} \Phi(t, r) - \frac{1}{r^2} \partial_r [r^2 g(r) \partial_r \Phi(t, r)] + \frac{\xi^2 + \frac{1}{4}}{r^2} \Phi \\ + m^2 \Phi(t, r) - \lambda^2 R_{\text{GB}}^2 \Phi = 0. \end{aligned} \quad (4.13)$$

In this scalar field equation there is a direct coupling of the scalar field to the GB term and also an extra parameter ξ appears because of the hyperbolic geometry.

Changing the variables to

$$\Phi(t, r) = \frac{\chi(t, r)}{r} \Rightarrow r^2 \partial_r \Phi = r\chi' - \chi \Rightarrow \partial_r(r^2 \partial_r \Phi) = r\chi'', \quad (4.14)$$

the scalar equation becomes

$$\partial_{tt}\chi - g(r) \frac{d}{dr} \left(g(r) \frac{d}{dr} \chi \right) + \frac{g(r)}{r} \frac{df(r)}{dr} \chi + g(r) \frac{\xi^2 + \frac{1}{4}}{r^2} \chi + m^2 g(r) \chi - \lambda^2 g(r) R_{\text{GB}}^2 \chi = 0. \quad (4.15)$$

Introducing tortoise coordinates

$$dr_* = \frac{dr}{g(r)} \Leftrightarrow g(r) \frac{d}{dr} = \frac{d}{dr_*}, \quad (4.16)$$

the equation takes the form

$$\partial_{tt}\chi - \frac{d^2}{dr_*^2} \chi + g(r) \left[\frac{1}{r} \frac{dg(r)}{dr} + \frac{\xi^2 + \frac{1}{4}}{r^2} + m^2 - \lambda^2 R_{\text{GB}}^2 \right] \chi = 0. \quad (4.17)$$

The time dependence of χ is $e^{-i\omega t}$ and the above equation takes the Schrödinger-like form

$$-\frac{d^2}{dr_*^2} \chi + g(r) V(r) \chi = \omega^2 \chi, \quad (4.18)$$

where the potential is given by

$$V(r) \equiv \frac{1}{r} \frac{dg(r)}{dr} + \frac{\xi^2 + \frac{1}{4}}{r^2} + m^2 - \lambda^2 R_{\text{GB}}^2. \quad (4.19)$$

For the TBH the potential becomes

$$V(r) = \frac{2}{L^2} + \frac{2M}{r^3} + \frac{\xi^2 + \frac{1}{4}}{r^2} + m^2 - \lambda^2 R_{\text{GB}}^2. \quad (4.20)$$

Setting

$$\chi = \psi_\omega e^{-i\omega r_*},$$

the scalar field equation becomes

$$g(r) \frac{d^2 \psi_\omega}{dr^2} + \left(\frac{dg(r)}{dr} - 2i\omega \right) \frac{d\psi_\omega}{dr} = V(r) \psi_\omega, \quad (4.21)$$

where $V(r)$ is given by (4.20). To investigate the properties of the scalar field, it is useful to change variables from r to $x = \frac{1}{r}$. We also define $h(x) = g(\frac{1}{x})$. Then Eq. (4.21) is transformed into

$$h(x) \left[x^4 \frac{d^2 \psi_\omega}{dx^2} + 2x^3 \frac{d\psi_\omega}{dx} \right] + \left(-x^2 \frac{dh(x)}{dx} - 2i\omega \right) \left[-x^2 \frac{d\psi_\omega}{dx} \right] = V(x) \psi_\omega, \quad h(x) = \frac{1}{L^2 x^2} - 2Mx - 1, \quad (4.22)$$

where

$$V(x) = \frac{2}{L^2} + 2Mx^3 + \left(\xi^2 + \frac{1}{4} \right) x^2 + m^2 - 24\lambda^2 \left[\frac{1}{L^4} + 2M^2 x^6 \right]. \quad (4.23)$$

The horizon variable x_+ is determined through

$$h(x_+) = 0 \Rightarrow \frac{1}{L^2 x_+^2} - 2Mx_+ - 1 = 0 \Rightarrow 2M = \frac{1}{L^2 x_+^3} - \frac{1}{x_+}. \quad (4.24)$$

This means that

$$h(x) = \frac{1}{L^2 x^2} - \left(\frac{1}{L^2 x_+^3} - \frac{1}{x_+} \right) x - 1 \Rightarrow \frac{dh(x)}{dx} = -\frac{2}{L^2 x^3} + \frac{1}{x_+}, \quad (4.25)$$

so that the metric function and the potential take the form

$$h(x) = (x - x_+) \frac{L^2 x^2 x_+^2 - x^2 - x_+^2 - x x_+}{L^2 x_+^3 x^2},$$

and

$$V(x) = \frac{2}{L^2} + 2Mx^3 + \left(\xi^2 + \frac{1}{4} \right) x^2 + m^2 - 24\lambda^2 \left[\frac{1}{L^4} + \frac{(1 - x_+^2)^2}{2x_+^6} x^6 \right]. \quad (4.26)$$

The introduction of the horizon radius in the scalar field equation will be helpful to study the behavior of the scalar field near and far away from the horizon of the black hole.

Equation (4.22) transforms into

$$x^4 h(x) \frac{d^2 \psi_\omega}{dx^2} + \left[2x^3 h(x) + x^4 \frac{dh(x)}{dx} + 2i\omega x^2 \right] \frac{d\psi_\omega}{dx} = V(x) \psi_\omega, \quad (4.27)$$

$$\frac{x^4 h(x)}{x - x_+} \frac{d^2 \psi_\omega}{dx^2} + \frac{1}{x - x_+} \left[2x^3 h(x) + x^4 \frac{dh(x)}{dx} + 2i\omega x^2 \right] \frac{d\psi_\omega}{dx} = \frac{(x - x_+) V(x)}{(x - x_+)^2} \psi_\omega. \quad (4.28)$$

We define

$$s(x) = \frac{x^4 h(x)}{x - x_+}, \quad t(x) = 2x^3 h(x) + x^4 \frac{dh(x)}{dx} + 2i\omega x^2,$$

$$u(x) = (x - x_+)V(x),$$

so that Eq. (4.28) may be written in the form

$$s(x) \frac{d^2 \psi_\omega}{dx^2} + \frac{t(x)}{x - x_+} \frac{d\psi_\omega}{dx} = \frac{u(x)}{(x - x_+)^2} \psi_\omega. \quad (4.29)$$

We expand ψ_ω about x_+

$$\psi_\omega(x) = \sum_k a_n(\omega)(x - x_+)^n, \quad (4.30)$$

as well as the functions $s(x)$, $t(x)$ and $u(x)$, according to the expressions

$$s(x) = \sum_k s_n(\omega)(x - x_+)^n, \quad t(x) = \sum_k t_n(\omega)(x - x_+)^n,$$

$$u(x) = \sum_k u_n(\omega)(x - x_+)^n. \quad (4.31)$$

Notice that $s(x)$ is a polynomial, since $h(x_+) = 0$.

Using the scalar field equation we find a recurrence formula of the form

$$a_n(\omega) = -\frac{1}{P_{n,0}} \sum_{m=n-7}^{n-1} P_{m,n-m} a_m(\omega),$$

$$P_{m,n-m} = m(m-1)s_{n-m} + mt_{n-m} + u_{n-m}. \quad (4.32)$$

For the consistency of our calculations we demand that the wave function vanishes at infinity ($r \rightarrow \infty$, $x = 0$), which yields the equation

$$\psi_\omega(0) = \sum_k a_n(\omega)(-x_+)^n = 0. \quad (4.33)$$

One has to solve the scalar field equation for ω , which are the quasinormal frequencies. We solve the scalar equation numerically and we plot the points of the complex ω plane, where $\psi_\omega(0)$ vanishes. The method we use is to make a contour plot for each of the real and imaginary parts of $\psi_\omega(0)$, that is, find the points where each of the above vanishes. The points that we are looking for are exactly the points of intersection of the various curves. We have used between 500 and 1000 terms in the above sums, the criterion being the stabilization of the results.

A. QNMs for $\lambda = 0.5$ and $\xi = 0$

As we saw in the analytic calculation, the system becomes unstable for large values of λ , larger than about 0.61. At first we will consider values safely below this value.

We will consider λ to take the value 0.5, where we do not expect instabilities. As can be seen in Fig. 4, left panel, the intersections of the curves for $r_+ = 1.10$ lie in the negative ω_I half-plane, the line connecting them has a negative slope and the consecutive imaginary parts differ by $2i$. As one considers larger black holes, that is, larger r_+ , the QNMs move toward less negative values: a relevant result is shown in Fig. 4, right panel, where $r_+ = 0.95$ and $r_+ = 1.60$; in addition, the differences between consecutive QNMs increase in magnitude, that is, the QNMs appear more sparse. At some value of r_+ the intersections disappear completely, a fact indicating that no QNMs exist for large black holes.

In Fig. 5, λ is set to the relatively large value $\lambda = 1.5$, ξ is set to 0 and r_+ takes on the values 1.10 and 2.00. For $r_+ = 1.10$ (left panel), apart from the QNMs with $\omega_I < 0$, there exist several QNMs with $\omega_I > 0$, signaling instability. It is conceivable that this instability means that the metric

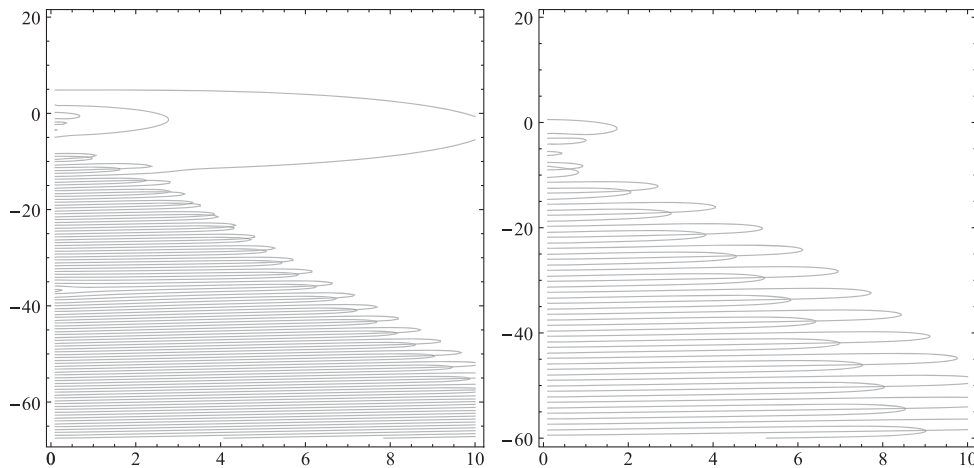
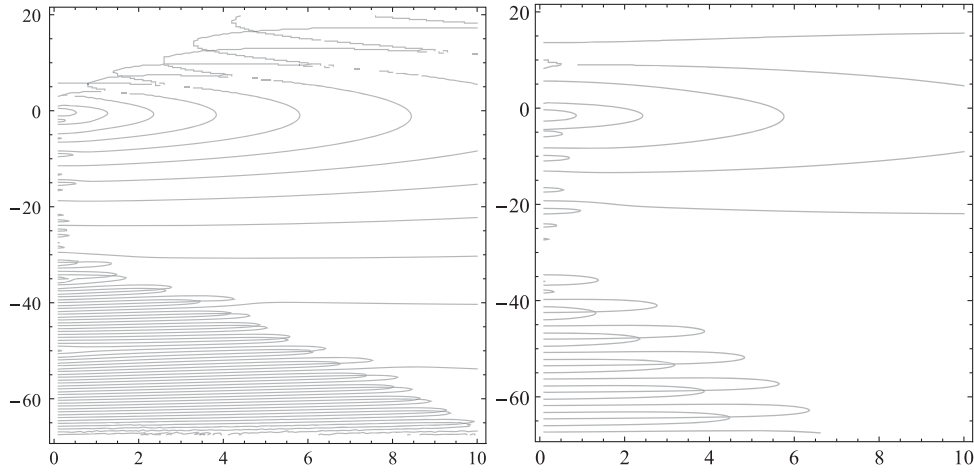


FIG. 4. $\lambda = 0.5$, $\xi = 0$, $r_+ = 1.10$, $r_+ = 1.60$.


 FIG. 5. $\lambda = 1.5$, $\xi = 0.0$, and $r_+ = 1.10, 2.00$.

used is no longer operational and scalarization should be considered. We note that the QNMs with $\omega_I > 0$ have a positive slope. The number of QNMs with $\omega_I > 0$ decreases as r_+ increases, until at $r_+ = 2.00$ (right panel) they disappear completely. If we keep increasing r_+ , even the QNMs with $\omega_I < 0$ disappear; this indicates once more that no QNMs exist for large black holes.

B. QNMs for $\xi = 0$, $r_+ = 1.10$ and large λ

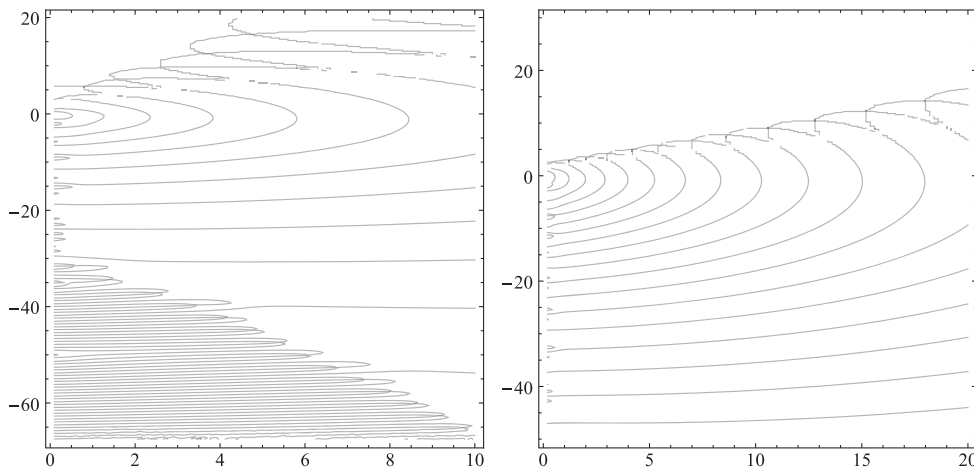
Figure 6 refers to the dependence of the QNMs on λ , when $\xi = 0$ and $r_+ = 1.10$. For $\lambda = 1.50$ (left panel, which is just a reproduction of Fig. 5 above), QNMs exist with negative ω_I . In addition QNMs with positive values of ω_I appear, whose existence gets more pronounced as λ increases. For $\lambda = 3.0$, the QNMs with negative ω_I disappear. This picture persists for even larger values of λ . This is consistent with the remark made earlier that the expression $\sqrt{9 - 24\lambda^2}$, appearing in the analytical treatment,

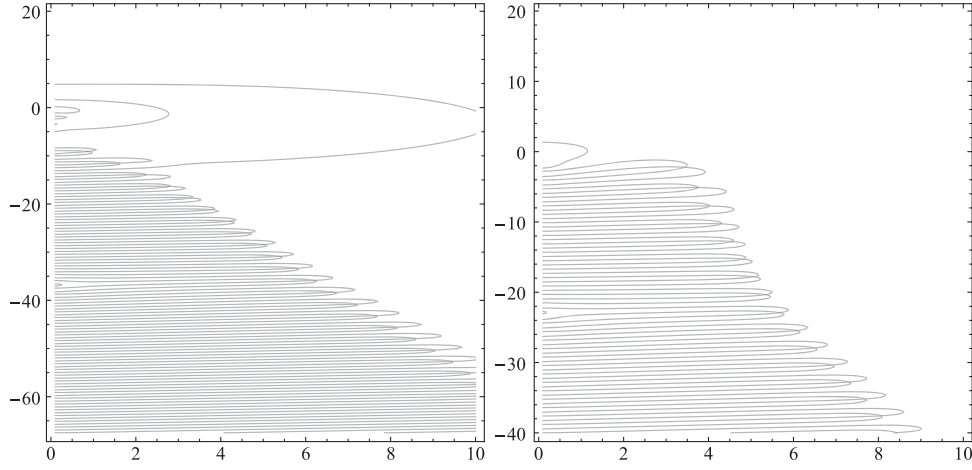
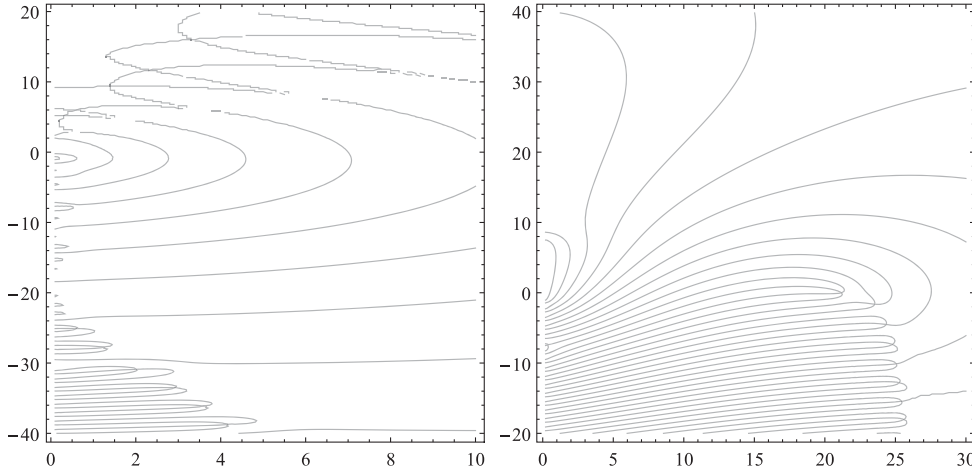
suggests that, for large values of λ , instabilities are expected to set in.

C. QNMs for $r_+ = 1.10$ and various values of ξ

Figure 7 contains the QNMs when $\lambda = 0.5$ is small, $r_+ = 1.10$ and ξ is set either to 0.0 or to 5.0. The left panel is the same as the left panel of Fig. 4. The influence of the value of ξ is apparent: the real parts of the QNMs move toward bigger positive values.

On the other hand, the influence of ξ is somewhat different when $\lambda = 1.5$, that is when it takes a moderately large value. The situation for $\xi = 0$ is depicted in Fig. 5, left panel. In Fig. 8, left panel, one may see the modifications brought about by the increasing values for ξ : when $\xi = 5.0$, a modest value, the QNMs with negative ω_I are not modified very much; on the contrary the QNMs with positive ω_I are influenced. The nature of this change becomes clear for the value $\xi = 30.0$, shown in Fig. 8,


 FIG. 6. $\xi = 0.0$, $r_+ = 1.10$, and $\lambda = 1.5$ (left), $\lambda = 3.0$ (right).


 FIG. 7. $\lambda = 0.50$, $r_+ = 1.10$, and $\xi = 0.0$ (left), $\xi = 5.0$ (right).

 FIG. 8. $\lambda = 1.50$, $r_+ = 1.10$, and $\xi = 5.0$ (left), $\xi = 30.0$ (right).

right panel: the QNMs with positive ω_I disappear completely, while the QNMs with negative ω_I move to less negative values. Once more, the real part of the QNMs moves to values of the order of ξ . Thus the unstable system depicted in Fig. 5, left panel, is transformed through the situation in Fig. 8, left panel, to the stable system shown in Fig. 8, right panel. Thus increasing the ξ value counterbalances the instability. In general, it seems that the parameters λ and ξ act competitively. Looking at this behavior another way, we find out that there is a critical value of ξ for each value of λ , such that below it the system is unstable.

V. CONCLUSIONS

In this work we studied the stability of a topological black hole in the presence of the coupling of a scalar field to the GB term in the ESTGB gravity theories and we investigated the possibility of its scalarization to

a MTZ-like black hole. We considered a gravity theory in the presence of a cosmological constant and a massive scalar field minimally coupled to gravity and also coupled to the GB term. We first considered possible tachyonic instabilities of these theories. Considering a general metric ansatz, we calculated the Klein-Gordon equation. Fixing the background metric to be the TBH we calculated the effective mass of the scalar field. A negative effective mass of the scalar field signals possible instabilities of the considered theory. To study the stability/instability of this theory we followed two approaches. We first calculated analytically the QNMs which can give us very important information on a stability of a theory. Then to verify our results we calculated also analytically the QNMs.

To study the QNM spectrum we performed scalar perturbations of a massive scalar field coupled to the GB term in the background of a topological-AdS black hole living in a hyperbolic spacetime expressed by the parameter ξ . The coupling of the scalar field to the GB term

is denoted by the parameter λ . For a fixed cosmological constant we have two competing effects. The first one is that, as λ is increasing, we expect the matter to interact more strongly with gravity, while as ξ is getting larger, the effects of the variations of the wave functions are dominant. Our goal was to see what are the effects of the increase of the strength of the parameters λ and ξ and their possible interplay on the stability of the topological black hole and if there are indications of a phase transition to a new scalarized black hole.

Calculating analytically the QNMs we found that for small black holes (we had fixed the horizon radius to $r_+ = 1$) we found a critical value of λ_c below which the topological black hole is stable under scalar perturbations. This can be seen in Fig. 1 where, for $\lambda < \lambda_c$, the real part of the QNMs is zero, while the imaginary part is negative. These results indicate that for values of λ below its critical value the topological black hole is stable under scalar perturbations. However, when the coupling constant λ is getting larger than its critical value, all of the QNMs develop a positive imaginary part signaling an instability of the background black hole. Calculating the scalar modes of the perturbations, we found that for large ξ the variations of the wave functions influences most effectively the behavior of the QNMs.

Then we calculated the QNMs for large black holes in the limit $r_+ \rightarrow +\infty$. Our analytical calculations showed that in this limit only nonphysical QNMs exist. Thus we concluded that only horizons around 1 may be expected to yield physical QNMs. We calculated also the scalar modes of the Klein-Gordon equation. As it was shown in Figs. 2 and 3 in the case of $\lambda > \lambda_c$, as λ is increasing there is evidence of a phase transition, i.e. to a topological black hole with scalar hair. Also when ξ is increasing this phase transition becomes more evident.

Calculating the QNMs of scalar perturbations numerically we get similar results for the instability of the background topological black hole. In a series of figures we showed that increasing the ξ value, for fixed value of λ

above its critical value, counterbalances the instability. In general, it seems that the parameters λ and ξ act competitively. Looking at this behavior another way, we find out that there is a critical value of ξ for each value of λ , such that below it the system is unstable. This is a very interesting result. It seems that the strength of the coupling of matter to curvature is strongly influenced by the geometry of the metric of the topological black hole and this leads to the stability/instability of the topological black hole and its scalarization.

To summarize our results, we found that there are critical values of the parameter λ , which is the coupling of matter to the GB term, and the parameter ξ which specifies the geometry of the background metric, which controls the instability of the topological black hole. Therefore we expect that the interplay of these parameters will lead to the scalarization of the topological black hole. To find the form of the scalarized topological black hole we have to allow the backreaction of the scalar field to the background topological black hole. We leave this for future work.

It would also be interesting to extend this study to rotating topological black holes. In [103] metrics with negative cosmological constant and representing rotating, topological black holes were discussed. By analytical continuation of the Kerr–de Sitter metric, a solution describing a rotating black hole whose event horizon is a Riemann surface of arbitrary genus was obtained. This solution has rotational symmetry and the amount of rotation it has is bounded by some power of the mass. More recently in [104] rotating Kerr-type black hole solutions were generated by the coupling of a pseudoscalar axion field coupled to topological Chern-Simons term. This coupling introduces a parameter expressing the rotation which appears in the metric of the black hole solution. In our case if our background metric is a rotating topological black hole, then except for the λ and ξ parameters another parameter will appear expressing the rotation of the black hole. It would be interesting to see the interplay of all these parameters on the stability of the rotating topological black hole.

-
- [1] B. P. Abbott *et al.* (LIGO Scientific and Virgo Collaborations), *Phys. Rev. Lett.* **116**, 061102 (2016).
 - [2] B. P. Abbott *et al.* (LIGO Scientific and Virgo Collaborations), *Phys. Rev. X* **9**, 031040 (2019).
 - [3] B. P. Abbott *et al.* (LIGO Scientific and Virgo Collaborations), *Astrophys. J. Lett.* **892**, L3 (2020).
 - [4] K. Akiyama *et al.* (Event Horizon Telescope Collaboration), *Astrophys. J.* **875**, L1 (2019).
 - [5] A. Joyce, B. Jain, J. Khoury, and M. Trodden, *Phys. Rep.* **568**, 1 (2015).
 - [6] S. Nojiri and S. D. Odintsov, eConf **C0602061**, 06 (2006) [arXiv:hep-th/0601213].
 - [7] T. Clifton, P. G. Ferreira, A. Padilla, and C. Skordis, *Phys. Rep.* **513**, 1 (2012).
 - [8] E. Berti *et al.*, *Classical Quantum Gravity* **32**, 243001 (2015).
 - [9] C. V. Vishveshwara, *Nature (London)* **227**, 936 (1970).
 - [10] K. D. Kokkotas and B. G. Schmidt, *Living Rev. Relativity* **2**, 2 (1999).
 - [11] E. Berti, V. Cardoso, and A. O. Starinets, *Classical Quantum Gravity* **26**, 163001 (2009).

- [12] P. O. Mazur and E. Mottola, [arXiv:gr-qc/0109035](#).
- [13] M. S. Morris, K. S. Thorne, and U. Yurtsever, *Phys. Rev. Lett.* **61**, 1446 (1988).
- [14] B. Holdom and J. Ren, *Phys. Rev. D* **95**, 084034 (2017).
- [15] V. Cardoso, E. Franzin, and P. Pani, *Phys. Rev. Lett.* **116**, 171101 (2016).
- [16] V. Cardoso, S. Hopper, C. F. B. Macedo, C. Palenzuela, and P. Pani, *Phys. Rev. D* **94**, 084031 (2016).
- [17] R. A. Konoplya and A. Zhidenko, *Rev. Mod. Phys.* **83**, 793 (2011).
- [18] Y. Fujii and K. Maeda, *The Scalar-Tensor Theory of Gravitation* (Cambridge University Press, Cambridge, England, 2007).
- [19] N. Bocharova, K. Bronnikov, and V. Melnikov, *Vestn. Mosk. Univ., Ser. 3: Fiz., Astron.* **6**, 706 (1970); J. D. Bekenstein, *Ann. Phys. (N.Y.)* **82**, 535 (1974); **91**, 75 (1975).
- [20] K. A. Bronnikov and Y. N. Kireev, *Phys. Lett.* **67A**, 95 (1978).
- [21] C. Martinez and J. Zanelli, *Phys. Rev. D* **54**, 3830 (1996).
- [22] M. Banados, C. Teitelboim, and J. Zanelli, *Phys. Rev. Lett.* **69**, 1849 (1992).
- [23] C. Martinez, R. Troncoso, and J. Zanelli, *Phys. Rev. D* **70**, 084035 (2004).
- [24] K. G. Zloshchastiev, *Phys. Rev. Lett.* **94**, 121101 (2005).
- [25] C. Martinez, R. Troncoso, and J. Zanelli, *Phys. Rev. D* **67**, 024008 (2003).
- [26] G. Dotti, R. J. Gleiser, and C. Martinez, *Phys. Rev. D* **77**, 104035 (2008).
- [27] T. Torii, K. Maeda, and M. Narita, *Phys. Rev. D* **64**, 044007 (2001).
- [28] E. Winstanley, *Found. Phys.* **33**, 111 (2003).
- [29] C. Martinez and R. Troncoso, *Phys. Rev. D* **74**, 064007 (2006).
- [30] T. Kolyvaris, G. Koutsoumbas, E. Papantonopoulos, and G. Siopsis, *Gen. Relativ. Gravit.* **43**, 163 (2011).
- [31] C. Charmousis, T. Kolyvaris, E. Papantonopoulos, and M. Tsoukalas, *J. High Energy Phys.* **07** (2014) 085.
- [32] T. Torii, K. Maeda, and M. Narita, *Phys. Rev. D* **59**, 064027 (1999).
- [33] T. J. T. Harper, P. A. Thomas, E. Winstanley, and P. M. Young, *Phys. Rev. D* **70**, 064023 (2004).
- [34] C. Martinez, J. P. Staforelli, and R. Troncoso, *Phys. Rev. D* **74**, 044028 (2006); C. Martinez and R. Troncoso, *Phys. Rev. D* **74**, 064007 (2006).
- [35] I. Z. Stefanov, S. S. Yazadjiev, and M. D. Todorov, *Mod. Phys. Lett. A* **23**, 2915 (2008).
- [36] D. D. Doneva, S. S. Yazadjiev, K. D. Kokkotas, and I. Z. Stefanov, *Phys. Rev. D* **82**, 064030 (2010).
- [37] V. Cardoso, I. P. Carucci, P. Pani, and T. P. Sotiriou, *Phys. Rev. Lett.* **111**, 111101 (2013).
- [38] V. Cardoso, I. P. Carucci, P. Pani, and T. P. Sotiriou, *Phys. Rev. D* **88**, 044056 (2013).
- [39] C. Herdeiro, E. Radu, N. Sanchis-Gual, and J. Font, *Phys. Rev. Lett.* **121**, 101102 (2018).
- [40] Y. Myung and De-Cheng Zou, *Eur. Phys. J. C* **79**, 273 (2019).
- [41] G. W. Horndeski, *Int. J. Theor. Phys.* **10**, 363 (1974).
- [42] T. Kolyvaris, G. Koutsoumbas, E. Papantonopoulos, and G. Siopsis, *Classical Quantum Gravity* **29**, 205011 (2012).
- [43] M. Rinaldi, *Phys. Rev. D* **86**, 084048 (2012).
- [44] T. Kolyvaris, G. Koutsoumbas, E. Papantonopoulos, and G. Siopsis, *J. High Energy Phys.* **11** (2013) 133.
- [45] E. Babichev and C. Charmousis, *J. High Energy Phys.* **08** (2014) 106.
- [46] A. Cisterna and C. Erices, *Phys. Rev. D* **89**, 084038 (2014).
- [47] G. Koutsoumbas, K. Ntorkis, E. Papantonopoulos, and M. Tsoukalas, *Phys. Rev. D* **95**, 044009 (2017).
- [48] A. Anabalón, A. Cisterna, and J. Oliva, *Phys. Rev. D* **89**, 084050 (2014).
- [49] A. Cisterna, T. Delsate, and M. Rinaldi, *Phys. Rev. D* **92**, 044050 (2015).
- [50] A. Cisterna, T. Delsate, L. Ducobu, and M. Rinaldi, *Phys. Rev. D* **93**, 084046 (2016).
- [51] K. S. Stelle, *Phys. Rev. D* **16**, 953 (1977).
- [52] J. Polchinski, *String Theory* (Cambridge University Press, Cambridge, England, 2001), Vols. 1 and 2.
- [53] S. Mignemi and N. R. Stewart, *Phys. Rev. D* **47**, 5259 (1993).
- [54] P. Kanti, N. E. Mavromatos, J. Rizos, K. Tamvakis, and E. Winstanley, *Phys. Rev. D* **54**, 5049 (1996).
- [55] T. Torii, H. Yajima, and K. i. Maeda, *Phys. Rev. D* **55**, 739 (1997).
- [56] D. Ayzenberg and N. Yunes, *Phys. Rev. D* **90**, 044066 (2014); **91**, 069905(E) (2015).
- [57] B. Kleihaus, J. Kunz, and E. Radu, *Phys. Rev. Lett.* **106**, 151104 (2011).
- [58] B. Kleihaus, J. Kunz, S. Mojica, and M. Zagermann, *Phys. Rev. D* **93**, 064077 (2016).
- [59] D. D. Doneva and S. S. Yazadjiev, *Phys. Rev. Lett.* **120**, 131103 (2018).
- [60] H. O. Silva, J. Sakstein, L. Gualtieri, T. P. Sotiriou, and E. Berti, *Phys. Rev. Lett.* **120**, 131104 (2018).
- [61] C. M. Chen, D. V. Gal'tsov, and D. G. Orlov, *Phys. Rev. D* **78**, 104013 (2008).
- [62] C. M. Chen, D. V. Gal'tsov, and D. G. Orlov, *Phys. Rev. D* **75**, 084030 (2007).
- [63] G. Antoniou, A. Bakopoulos, and P. Kanti, *Phys. Rev. Lett.* **120**, 131102 (2018).
- [64] G. Antoniou, A. Bakopoulos, and P. Kanti, *Phys. Rev. D* **97**, 084037 (2018).
- [65] Y. Myung and De-Cheng Zou, *Phys. Rev. D* **98**, 024030 (2018).
- [66] D. D. Doneva, S. Kiorpelidi, P. G. Nedkova, E. Papantonopoulos, and S. S. Yazadjiev, *Phys. Rev. D* **98**, 104056 (2018).
- [67] C. A. R. Herdeiro and E. Radu, *Phys. Rev. D* **99**, 084039 (2019).
- [68] H. O. Silva, J. Sakstein, L. Gualtieri, T. P. Sotiriou, and E. Berti, *Phys. Rev. Lett.* **120**, 131104 (2018).
- [69] M. Minamitsuji and T. Ikeda, *Phys. Rev. D* **99**, 044017 (2019).
- [70] H. O. Silva, C. F. B. Macedo, T. P. Sotiriou, L. Gualtieri, J. Sakstein, and E. Berti, *Phys. Rev. D* **99**, 064011 (2019).
- [71] N. Andreou, N. Franchini, G. Ventagli, and T. P. Sotiriou, *Phys. Rev. D* **99**, 124022 (2019).
- [72] M. Minamitsuji and T. Ikeda, *Phys. Rev. D* **99**, 104069 (2019).
- [73] Y. Peng, *Phys. Lett. B* **807**, 135569 (2020).

- [74] H. S. Liu, H. Lu, Z. Y. Tang, and B. Wang, *Phys. Rev. D* **103**, 084043 (2021).
- [75] D. D. Doneva, K. V. Staykov, S. S. Yazadjiev, and R. Z. Zheleva, *Phys. Rev. D* **102**, 064042 (2020).
- [76] D. Astefanesei, C. Herdeiro, J. Oliveira, and E. Radu, *J. High Energy Phys.* **09** (2020) 186.
- [77] P. Cañate and S. E. Perez Bergliaffa, *Phys. Rev. D* **102**, 104038 (2020).
- [78] C. L. Hunter and D. J. Smith, [arXiv:2010.10312](https://arxiv.org/abs/2010.10312).
- [79] A. Bakopoulos, G. Antoniou, and P. Kanti, *Phys. Rev. D* **99**, 064003 (2019).
- [80] Y. Brihaye, C. Herdeiro, and E. Radu, *Phys. Lett. B* **802**, 135269 (2020).
- [81] A. Bakopoulos, P. Kanti, and N. Pappas, *Phys. Rev. D* **101**, 044026 (2020).
- [82] A. Bakopoulos, P. Kanti, and N. Pappas, *Phys. Rev. D* **101**, 084059 (2020).
- [83] K. Lin, S. Zhang, C. Zhang, X. Zhao, B. Wang, and A. Wang, *Phys. Rev. D* **102**, 024034 (2020).
- [84] Y. Brihaye, B. Hartmann, N. P. Aprile, and J. Urrestilla, *Phys. Rev. D* **101**, 124016 (2020).
- [85] H. Guo, S. Kiorpelidi, X. M. Kuang, E. Papantonopoulos, B. Wang, and J. P. Wu, *Phys. Rev. D* **102**, 084029 (2020).
- [86] Z. Y. Tang, B. Wang, T. Karakasis, and E. Papantonopoulos, *Phys. Rev. D* **104**, 064017 (2021).
- [87] H. Guo, X. M. Kuang, E. Papantonopoulos, and B. Wang, *Eur. Phys. J. C* **81**, 842 (2021).
- [88] G. Koutsoumbas, S. Musiri, E. Papantonopoulos, and G. Siopsis, *J. High Energy Phys.* **10** (2006) 006.
- [89] G. Koutsoumbas, E. Papantonopoulos, and G. Siopsis, *J. High Energy Phys.* **05** (2008) 107.
- [90] G. Koutsoumbas, E. Papantonopoulos, and G. Siopsis, *Classical Quantum Gravity* **26**, 105004 (2009).
- [91] C. Vlachos, E. Papantonopoulos, and K. Destounis, *Phys. Rev. D* **103**, 044042 (2021).
- [92] J. P. S. Lemos and V. T. Zanchin, *Phys. Rev. D* **54**, 3840 (1996); J. P. S. Lemos, *Phys. Lett. B* **353**, 46 (1995).
- [93] R. B. Mann, *Classical Quantum Gravity* **14**, L109 (1997); *Nucl. Phys.* **B516**, 357 (1998).
- [94] L. Vanzo, *Phys. Rev. D* **56**, 6475 (1997).
- [95] D. R. Brill, J. Louko, and P. Peldan, *Phys. Rev. D* **56**, 3600 (1997).
- [96] D. Birmingham, *Classical Quantum Gravity* **16**, 1197 (1999).
- [97] G. Gibbons and S. A. Hartnoll, *Phys. Rev. D* **66**, 064024 (2002).
- [98] D. Birmingham and S. Mokhtari, *Phys. Rev. D* **76**, 124039 (2007).
- [99] B. Wang, E. Abdalla, and R. B. Mann, *Phys. Rev. D* **65**, 084006 (2002).
- [100] R. Aros, C. Martinez, R. Troncoso, and J. Zanelli, *Phys. Rev. D* **67**, 044014 (2003).
- [101] D. Birmingham and S. Mokhtari, *Phys. Rev. D* **74**, 084026 (2006).
- [102] F. Sbisà, *Eur. J. Phys.* **36**, 015009 (2015).
- [103] D. Klemm, V. Moretti, and L. Vanzo, *Phys. Rev. D* **57**, 6127 (1998).
- [104] N. Chatzifotis, P. Dorlis, N. E. Mavromatos, and E. Papantonopoulos, *Phys. Rev. D* **105**, 084051 (2022).